ORIGINAL ARTICLE

Enhancement of thermal comfort in a large space building

Haslinda Mohamed Kamar [a,*], N.B. Kamsah [a], F.A. Ghaleb [a], M. Idrus Alhamid [b]

[a] *School of Mechanical Engineering, Faculty of Engineering, Universiti Teknologi Malaysia, Johor Bahru, 81310 Skudai, Malaysia*
[b] *Departemen Teknik Mesin, Fakultas Teknik, Universitas Indonesia, Kampus Baru – UI, Depok 16424, Indonesia*

Abstract Many large confined spaces in tropical countries employ a combination of natural ventilation and mechanical fans for space cooling purposes. However, due to low wind velocity and an inability of mechanical fans to remove warm air, this cooling method is not capable of providing a satisfactory thermal comfort to the occupants. This study aims to find out a simple strategy for improving the thermal comfort inside a mosque building in Malaysia. Field measurements were first carried out to acquire the airflow velocity, air temperature, relative humidity and mean radiant temperature inside the mosque, for a duration of one-year. These data were then used to calculate two thermal comfort indices namely predicted mean vote (PMV) and predicted the percentage of dissatisfied (PPD). A computational fluid dynamic (CFD) method was employed to predict airflow and temperature distributions and to examine the effects of installing exhaust fans on the thermal comfort condition inside the mosque. Parametric flow analyses were conducted to find out the arrangement of the exhaust fans that would produce highest improvement in the PMV and PPD thermal comfort indices. It was found that, under the present ventilation condition, both PMV and PPD values at the selected locations inside the mosque exceed the respective upper limits as recommended in the ASHRAE Standard-55, indicating that the thermal comfort inside the mosque is extremely hot. Results of parametric flow analyses show that installing ten exhaust fans with a 1-m diameter at the south-side wall, at the height of 6 m from the floor, has a potential of reducing the PMV index by 75–95% and the PPD index by 87–91%. This translates into a vast improvement in the thermal comfort inside the mosque building.

1. Introduction

Large buildings such as industrial buildings, aircraft hangars, sports halls, mosques, and stadiums exist in many places worldwide. The remarkable issues that frequently arise in such structures are energy consumptions, indoor air quality and thermal comfort [1–8] and mosques are no exception. A mosque is a place for Muslims to perform their religious activities.

* Corresponding author.
E-mail addresses: haslinda@utm.my (H. Mohamed Kamar), nazrikh@utm.my (N.B. Kamsah), mamak@eng.ui.ac.id (M. Idrus Alhamid).
Peer review under responsibility of Faculty of Engineering, Alexandria University.

Due to many occupants inside the mosque, thermal comfort is a requirement to ensure the tranquillity of the occupants when conducting their activities. The thermal comfort study inside mosques has not been widely carried out by other researchers [2,11–13]. Therefore, there is a need to conduct such studies for the benefit of the occupants.

In general, the poor thermal comfort level usually will lead to less productivity, health decline and little thermal satisfaction of the occupants. Thermal comfort can be defined as ''a condition of mind which expresses satisfaction with the thermal environment'' [11,12]. According to Fanger [12], thermal comfort can be evaluated by assessing six main parameters, in which four of them are related to the surrounding while the other two are associated with the people. The surrounding parameters include the air relative humidity (RH), air temperature, (T_a), airflow velocity (V_a) and mean radiant temperature (T_{mrt}), while the people parameters include their clothing type and activity levels. Ventilation improves the thermal comfort level of occupied areas by providing a heat transport mechanism and lowering the air temperature [5]. There are several types of ventilation method that can be employed for controlling the air distribution and giving a satisfactory level of thermal comfort inside a building such as natural, mechanical, and hybrid ventilation [13]. The natural ventilation uses natural forces which originate from nearby airflow to promote and displace the air through specified openings such as doors and windows [14]. The mechanical ventilation employs mechanical devices such as fans and exhaust vents for supplying and removing the air [15]. While, the hybrid ventilation adopts both natural and mechanical ventilation methods for providing thermal comfort [1,16]. The commonly used method to provide thermal comfort in Malaysia mosques is by using natural ventilation and mechanical fans [17,18]. However, as Malaysia experiences a low wind velocity, specifically on average around 1.5 m/s [19], and the limitation of mechanical fans of removing the warm air [2,21–27], the current ventilation method is not suitable to be used in a large space building. Due to that, an alternative strategy for the ventilation method is necessary for providing a satisfactory level of thermal comfort in a large area building such as inside the mosque [27].

Various performance criteria have been developed to assess the level of thermal comfort inside occupied buildings. Among others is the Effective Temperature Index, Equatorial Comfort Index, Predicted Mean Vote (PMV), Predicted Percentage Dissatisfied (PPD), and Corrected Effective Temperature (CET) index [28]. However, most of those indices have limitations in their applications since they are based on specific climatic conditions. But, an exception is to the Predicted Mean Vote (PMV) and the Predicted Percentage Dissatisfied (PPD). They are widely used to represent the thermal comfort in many types of working spaces [2,3,29,30]. The PMV is defined as an index to predict the mean value of the votes of a large group of persons on the seven points of thermal sensation scale [11,31]. The PPD index represents the percentage of individuals who felt more than slightly warm or slightly cold [32].

There are several methods used to examine the ventilation effectiveness of buildings. The commonly used techniques are empirical models, analytical models, zonal models, multizone models, small-scale experimental models, full-scale experimental models, and computational fluid dynamics (CFD) [5]. Based on the literature, the CFD method was found to be a more attractive approach, since it gives reliable results in predicting ventilation parameters and the advancement in digital computing [5,33,34]. Besides, CFD and experimental approaches have been employed in many studies to investigate the indoor thermal comfort in buildings [3,30,36–48].

This article presents a study on improving thermal comfort inside the main hall of a mosque located in Johor Bahru, Malaysia, using a combination of field measurement and computational fluid dynamics (CFD) numerical method. The primary goal is to find the most suitable installation arrangement of exhaust fans that would improve the thermal comfort inside the hall. The thermal comfort was evaluated based on calculated values of PMV and PPD indices. These indices were calculated based on a widely accepted method that was described by Fanger [48] and has been adopted in the ISO standard.

2. Methodology

2.1. Field measurement

A field measurement was conducted on a selected mosque building that is in Johor Bahru, Malaysia. Fig. 1(a) shows the exterior view of the building while Fig. 1(b) shows the interior space of the main hall. The length, width, and height of the hall are 35 m, 30 m, and 12 m, respectively. It can accommodate about 1270 occupants. The walls on the right and left sides of the hall are furnished with 12 doors, while the wall at the back side has ten doors. The doors have dimensions of 1.4 m width and 2.2 m in height. Windows are placed above all the doors, and each has dimensions of 1.4 m width and 1.6 m in height. The doors are left in open when there are occupants. This is to provide a natural flow of outside air into the main hall. Besides, the hall is furnished with 28 units of wall fans and 20 units of stand fans, to promote a better airflow inside the hall.

The purpose of the field measurement is to obtain the values of parameters required to calculate the PMV and PPD indices, which represent the state of thermal comfort inside the main hall. The parameters are airflow velocity, air temperature, mean radiant temperature and air relative humidity. They are also used as the boundary conditions for the CFD flow analyses and for validating the CFD model. The parameters were acquired at five chosen locations inside the hall. These locations are indicated by points P1 to P5 in Fig. 2(a). At each location, the probe of the measuring instrument was placed at the height of 1.1 m from the floor [11], as shown in Fig. 2(b). This height represents an average breathing level of the occupants when they are in a standing position.

The field measurement was carried out for a one-year period, i.e., from October 2014 to September 2015. The data collection was conducted from 11:30 am to 3:00 pm, i.e., when the hall was nearly fully occupied. The data were recorded at every 10-minute interval during this period. The instruments used were hot wire anemometer for measuring airflow velocity and temperature & humidity recorder to acquire air temperature and humidity. These instruments were wire-connected to a data logger to allow the acquired data to be stored safely. The instruments are shown in Fig. 3, and their accuracy is given in Table 1. The instruments were carefully calibrated before being used. An uncertainty analysis was performed to estimate the accuracy range of the acquired data. Table 2

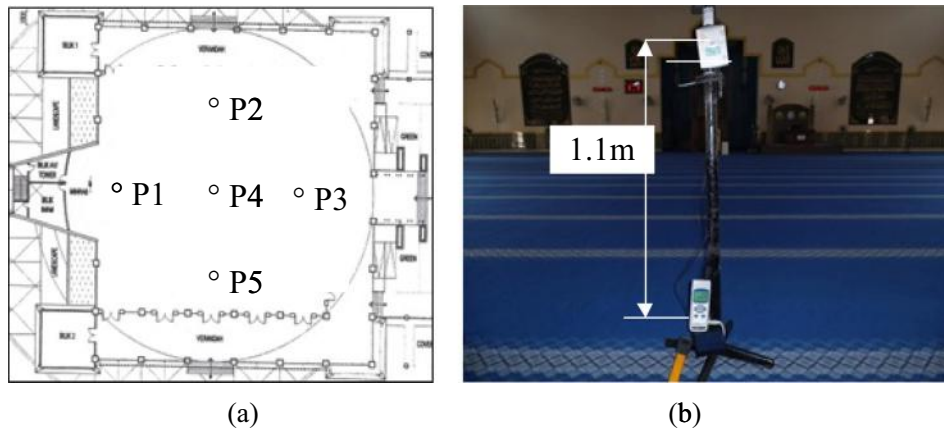Fig. 1 (a) The mosque building and (b) the main hall.

Fig. 2 (a) Locations of data collection locations (P1 to P5) inside the mosque, and (b) placement of a measuring instrument and its probe.

Fig. 3 (a) Hot wire anemometer; (b) temperature & humidity recorder; and (c) HOBO UX120 data logger.

Table 1	Accuracy of the measuring instruments.		
Parameters	Measuring instrument	Model	Accuracy
Air velocity	Hot wire anemometer	HHF-SD1	$\pm 15\%$
Air temperature			$\pm (0.4\% + 0.5\,°C)$
Relative humidity	Temperature & humidity recorder	H14-001	$\pm 3.5\%$
Surface wall temperature	HOBO Series data logger	UX120	$\pm 0.21\,°C$

Table 2 Uncertainties of the measured parameters.

Types of analysis	Air parameters		
	Air temperature (°C)	Air velocity (m/s)	Relative humidity (%)
Minimum (y)	31.2	0.49	67.25
Maximum (X)	31.8	0.62	70.32
Mean ($\bar{X}$)	31.45	0.53	68.97
Standard deviation (σ)	0.17	0.05	1
Standard uncertainty [$(X + \sigma)$ and $(X - \sigma)$]	31.8 ± 0.17	0.62 ± 0.5	70.32 ± 1.0
Relative standard uncertainty (σ/X)	0.01	0.8	0.014
Expanded uncertainty ($U = \sigma K$)	0.34	0.1	2.0
Standard error (α)	0.26	0.3	0.0

shows the uncertainties of the airflow velocity, air temperature and relative humidity obtained from the field measurement.

2.2. Calculation of thermal comfort indices

The thermal comfort inside the mosque was assessed based on two indices, i.e., predicted mean vote (PMV) and percent of people dissatisfied (PPD). The PMV is an empirical index that was developed based on a steady-state model of thermal exchanges between the human body and the environment [48]. It predicts the mean response of a large group of people according to the ASHRAE thermal sensation scale. The recommended range of PMV as stipulated in the ASHRAE Standard-55 [18] is between −0.5 and +0.5 for an interior space. The PPD on the other hand, predicts the percentage of occupants who are unsatisfied with the thermal conditions inside the space they are in. The PMV can be determined using Eq. (1) as follows [48],

$$PMV = [0.303 \exp(-0.036M) + 0.028] \times L \quad (1)$$

where

$$
\begin{aligned}
L = (M - V) &- 3.96 \times 10^{-8} f_{cl} \left[(t_{cl} + 273)^4 - (t_r + 273)^4 \right] \\
&- f_{cl} h_c (t_{cl} - t_a) - 3.05[5.73 - 0.007(M - W) - p_a] \\
&- 042[(M - W) - 58.15] - 0.0173M(5.87 - p_a) \\
&- 0.0014M(34 - t_a)
\end{aligned}
\quad (2)
$$

in which L is the thermal load on a human body (W/m²); M is the metabolic rate of a human body (W/m²), W is the rate of mechanical work done by a person (W/m²), t_a is the air temperature, t_r is the mean radiant temperature, f_{cl} is the clothing area factor, t_{cl} is the mean temperature of the outer surface of the clothed body, h_c is the convective heat transfer coefficient (W/m² °C), and p_a is the water vapour pressure in ambient air (kPa). The clothing temperature t_{cl} was found by iteration using the following relation,

$$
\begin{aligned}
t_{cl} = 35.7 - 0.028(M - W) \\
- R_{cl} \Big\{ 39.6 \times 10^{-9} f_{cl} \left[(t_{cl} + 273)^4 - (t_r + 273)^4 \right] + f_{cl} h_c (t_{cl} - t_a) \Big\}
\end{aligned}
\quad (3)
$$

where R_{cl} is the thermal resistance of clothing (m². °C/W). The predicted percentage dissatisfied (PPD) is a function of PMV and is given by,

$$PPD = 100 - 95e^{\left[-\left(0.335PMV^4 + 0.2179PMV^2 \right) \right]} \quad (4)$$

where e is Euler's number which has a nominal value of 2.718.

2.3. Computational fluid dynamic analysis

Computational fluid dynamic (CFD) method was employed in this study to predict the distribution of airflow velocity, air temperature and humidity at the data collection locations inside the hall, under the present ventilation condition and when exhaust fans were virtually installed at the hall envelope. The results were then used to calculate the thermal comfort indices at these locations. The indices were then compared with the corresponding values determined based on data obtained from the field measurement. ANSYS FLUENT CFD software was used to develop the computational domain based on the geometry of the mosque's hall and to perform all flow analyses. A parametric study was carried out to examine the effects of installing exhaust fans at different locations of the hall envelope, on the thermal comfort indices. The goal was to find out the suitable number of fans to use and their location that would give the best improvement in the thermal comfort indices inside the hall. The CFD flow analysis involves the following steps: construction of a simplified model of the hall (the computational domain), meshing the model, prescribing the boundary conditions, choosing a suitable air flow model based on the Reynolds Average Navier-Stoke (RANS) family models, setting the solution methods, and finally specifying the convergence criteria of the solution. The analyses were carried out in a transient mode until a satisfactory convergence of all the residuals was attained.

2.3.1. Simplified geometry of the mosque's hall

A simplified geometry of the mosque's hall space was developed using the ANSYS Fluent CFD software based on the actual dimensions of the hall, as shown in Fig. 4. This is con-
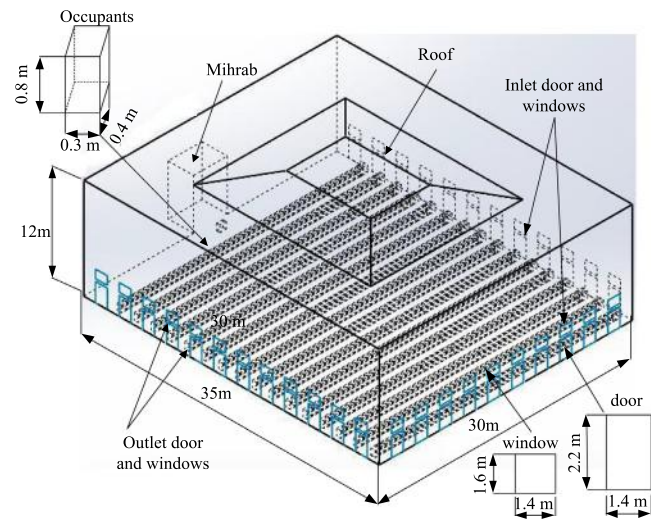
Fig. 4 Simplified CFD geometry of the mosque's hall (the computational domain).

sidered as the baseline CFD model, which is under the present ventilation condition. The length, width, and height of the hall are 35-m, 30-m, and 12-m, respectively.

Several simplifications were made on the geometry, which includes the exclusion of the furniture, the lamps, the wall fans, the standing fans and the minaret. The following features were included into the geometry: 1270 occupants, represented by square-shaped features, 12 doors on the right- and left side walls of the hall and 10 doors on the rear-side wall. Windows are also included in the geometry, located above all the doors. The dimensions of the doors are 1.4 m width and 2.2 m in height while for the windows are 1.4 m width and 1.6 m in height. The features representing the occupants have dimensions of 0.4 m width and 0.3 m thick. They are arranged in a sitting position with a height of 0.8 m, with a lateral spacing of 5 cm between them.

2.3.2. Meshing of the hall geometry

The interior space of the mosque (the hall) which represents the computational domain for the CFD flow analysis was meshed using *CutCell* elements and is illustrated in Fig. 5. It is a Cartesian meshing method that performs patch independent volume meshing and utilises advanced size functions. Finest elements were constructed in regions close to the doors and windows where there are inflows of outside air, while medium element was used in the regions adjacent to these areas. Coarse elements were used in the remaining areas of the computational domain. This meshing strategy could help reduce computational time during CFD flow analyses [33,34].

2.3.3. Boundary conditions

Realistic boundary conditions are an essential requirement in a CFD flow analysis. In this study, the following boundary conditions were prescribed on the baseline CFD model of the mosque. An inward airflow velocity of 0.3 m/s was specified at all the doors on the rear-side wall while an inward airflow velocity of 0.5 m/s was specified at all the doors on the right-side wall of the hall. An inward airflow velocity of 0.2 m/s was also specified at all windows on the rear-side wall while an inward airflow velocity of 0.4 m/s was specified at all windows on the right-side wall. Mass fraction of water vapour, $f_{water\ vapour}$ of 0.019 was prescribed at all doors and windows located at the right- and back-sides walls of the hall. An average air temperature of 28 °C was specified for all the incoming flowing air.

All airflow velocities were specified in a direction normal to all surfaces representing the doors and windows. A zero-gauge pressure (i.e., at atmospheric pressure of 100 kPa) was prescribed at all the doors and windows on the left-side wall of the hall. Mean radiant temperatures of different magnitudes were prescribed on surfaces of the roof, ceiling, walls, and floor of the hall, which were set as fixed boundaries. A no-slip boundary condition was prescribed on all these surfaces. Uniform temperature of 37 °C and heat generation at a rate of 15 W/m^3 were specified on all features of the occupants. To simplify the CFD flow simulation, it was assumed that the breathing by occupants does not affect the airflow pattern inside the hall and the magnitudes of the measured airflow velocity at all data collection locations. Furthermore, the probes for measuring the airflow velocities were set at the height of 1.1-m from the floor, which is much higher than the breathing level of the occupants that are in their sitting position. Table 3 lists the boundary conditions imposed on the baseline CFD model of the hall. The properties of air, water vapour, concrete material and the occupants were all obtained from the ASHRAE Standard-55 [9] and are shown in Table 4.

2.3.4. Solver, solution methods and convergence

A pressure-based solver was chosen as a solution method for the CFD flow analyses. This solver is generally applicable for a wide range of flow regimes, from low-speed incompressible flow to high-speed compressible flow. This solver requires less memory for data storage and allows flexibility in the solution procedure. A second-order upwind interpolation method was chosen to give results that are accurate to two decimal places. However, it uses larger stencils for second-order accuracy of the simulation results. This is generally essential with tetrahedral meshing or when the flow direction is not aligned with the grid. A pressure-velocity coupling solution approach was chosen in this study. The term pressure-velocity coupling refers to a numerical algorithm which uses a combination of continuity and momentum equations to derive an equation for pressure (or pressure correction) when using the pressure-based solver. The default solution scheme for this algorithm called a semi-implicit method for pressure-linked equations (SIMPLE) was selected due to its robustness. A sufficient number of iterations was specified to ensure acceptable convergence of the CFD solutions. At convergence, all discrete
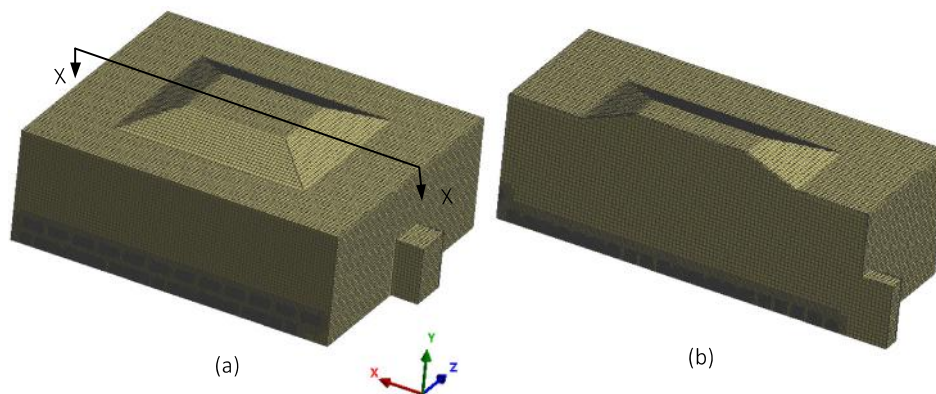

Fig. 5 Meshing of the computational domain: (a) a full hall geometry, and (b) a half-cut view through section X-X.

Table 3 The boundary conditions prescribed on the baseline CFD model.

Boundary conditions	Sections		Parameters
Inlet air	Right doors and windows		$V_{a,\,door} = 0.5$ m/s $V_{a,\,wind} = 0.4$ m/s $T_a = 28.2$ °C $f_{water\,vapour} = 0.019$
	Back doors and windows		$V_{a,\,door} = 0.3$ m/s $V_{a,\,wind} = 0.2$ m/s $T_a = 28.2$ °C $f_{water\,vapour} = 0.019$
Outlet air	Left door and window		Pressure = 0 Pa (gauge)
Temperature	Wall	Roof	$T_{w,r} = 34.4$ °C
		Ceiling	$T_{w,c} = 31.8$ °C
		Front	$T_{w,\,front} = 28.8$ °C
		Rear	$T_{w,\,rear} = 29.5$ °C
		Right	$T_{w,R} = 29$ °C
		Left	$T_{w,l} = 29.2$ °C
		Mihrab	$T_{w,M} = 29.4$ °C
		Floor	$T_{w,F} = 28$ °C
Temperature	Occupants		37 °C
Metabolic rate			150 W
Heat generation rate			15 W/m^3

conservation equations (momentum, energy, etc.) are obeyed in all cells or elements to a specified tolerance or the solution no longer changes with subsequent iterations. This means overall mass, momentum, energy, and scalar balances are achieved during the flow analysis. The convergence of The CFD solutions was monitored using a residual history, which represents the differences in the value of the desired quantity between two iterations. In general, a decrease in residuals by three orders of magnitude indicates at least a qualitative convergence. At this point, the primary flow features should have been established. In this study, absolute values of residuals for all the governing equations were set as 10^{-4} except for the energy equation, where the residual value was set to 10^{-6} as required when a pressure-based solver is used. A residual history plot during the flow analysis on the baseline CFD model of the hall is shown in Fig. 6, with iterations of 1500.

2.3.5. Selection of turbulent flow model

Choosing a suitable turbulent flow model is essential to ensure that a realistic CFD solution is attained for airflow distribution inside an enclosed space. In this study, the airflow inside the mosque interior space, i.e., the hall was assumed to be in

unsteady and irregular (aperiodic) motion in which the mass, momentum, as well as temperature, varies in time and space. Also, the airflow velocity was assumed to exhibit random variations in both magnitude and direction. Such assumptions allow for turbulence flow simulation to be carried out. Although several turbulent flow models are available in ANSYS Fluent software, the Reynolds-Averaged Navier-Stokes (RANS) family models were considered in this study because it is widely used models for simulations of airflow in confined spaces. The two-equation RANS model available in ANSYS Fluent are Standard k-ε, RNG k-ε, Realizable k-ε, Standard k-ω and the SST k-ω models. In this study series of tests were conducted to find out which of these flow models is the most suitable to use. The flow model tests were carried out according to the following steps. A flow simulation was carried out on the baseline CFD model by employing the Standard k-ε flow model. The boundary conditions described in Section 2.3.3 were specified on the CFD model, and the solution approach described in Section 2.3.4 was employed. A turbulence intensity of 4% was specified at all locations where there are inwards airflows. Turbulence intensity ranging from 1% to 5% is considered sufficient for modeling airflow inside an indoor environment [9]. From the flow simulation results, the airflow velocities and air temperatures at the five data collection locations inside the mosque were observed. Then their magnitudes were compared to the corresponding values obtained from the field measurement, for April 2015. Data for this month were chosen because they represent the highest throughout the year. The flow simulation was then repeated using other turbulent models, and the same steps were repeated. The results of the tests were presented in the form of bar chart plots. Fig. 7 shows plots of air temperatures at five data collection locations inside the hall while Fig. 8 shows similar plots of the airflow velocities. These air temperatures and airflow velocities were compared with the corresponding values obtained from the field measurement, at the same locations. It can be observed from both figures that the SST k-ω flow model produces air temperatures and airflow velocities that are closest to the corresponding field measurement magnitudes, at nearly all the data collection locations. Hence this flow model was employed in all the proceeding CFD flow simulations. A species transport model was adopted to simulate the transport of water vapour in the air and predict the distribution of air humidity inside the mosque interior building.

2.3.6. Grid independent test

A grid independent test was carried out on the baseline CFD model of the mosque. The purpose of this test is to determine the suitable number of elements that would have a negligible error on the outcomes of the flow simulation. This was done

Table 4 Properties of air, water vapour, concrete and features of occupants [11].

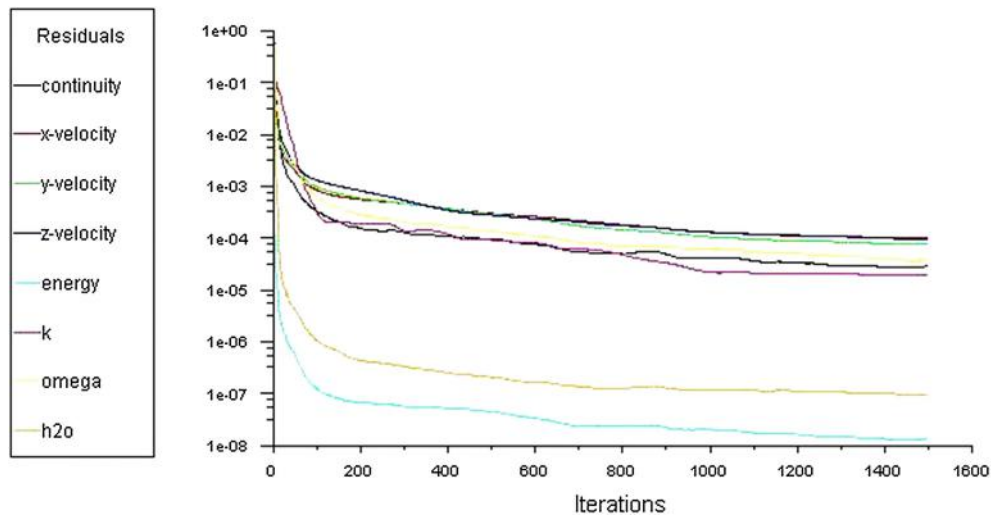| Properties	Air at 28.2 °C	Water vapour at 28.2 °C	Concrete	Occupant
Density (kg/m^3)	1.134	0.023	2400	985
Thermal conductivity (W/m K)	0.0262	0.0198	0.9	0.45
Specific heat (J/kg K)	1006.4	1872.6	0.75	2500
Molecular weight (kg/kg mol)	28.69	18.02	–	–
Specific gas constant (J/kg K)	287.1	461.9	–	–
Viscosity (kg/m s)	1.86321×10^{-5}	0.92982×10^{-5}	–	–

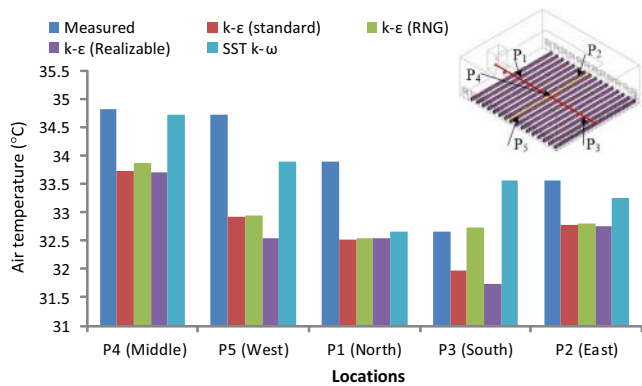**Fig. 6** A residual history plot during the CFD flow analysis.

Fig. 7 Air temperatures at all data collection locations for various turbulent flow models and comparison with the field measurement data.
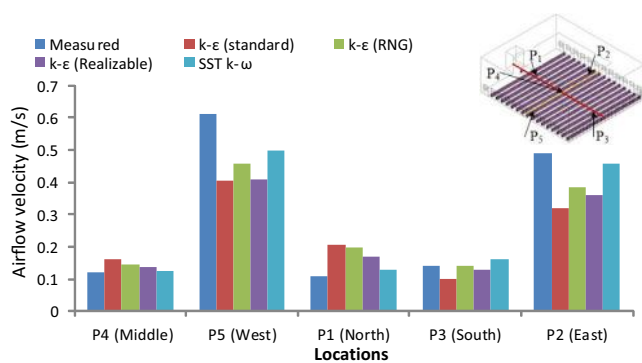

Fig. 8 Airflow velocities at all data collection locations for various turbulent flow models and comparison with the field measurement data.

by carrying out flow simulation on the baseline CFD model with boundary conditions as described in Section 2.3.3 and solution setup as described in Section 2.3.4. The *SST k-ω* flow model was employed throughout this test. The CFD model

with a coarse meshing of 1,072,752 elements was first employed. From the result of this simulation, the airflow velocity and air temperature at the five data collection locations inside the mosque were observed. The same simulation was repeated on the same CFD model but with increasingly finer meshing and similar results at the same locations were observed. The test was stopped when no significant variations in the airflow velocity and air temperature were observed at all the locations, with further meshing refinement. Results of this test are presented in the form of histogram plots. Fig. 9 shows such plots for the airflow velocity and Fig. 10 shows the same for the air temperature. It can be observed from these figures that meshing with 2,798,544 elements is adequate to ignore the error due to meshing on the flow simulation results.

2.3.7. Grid convergence index

In addition to the grid independent study, a grid convergence index (GCI) was also evaluated for the CFD model of the mosque. This index represents an error band on how far the computational solutions deviate from their respective asymptotic values. In many cases, the GCI values of less than 5% can be considered as satisfactory [36]. In this study, the GCI was determined based on the method described by Hajdukiewicz
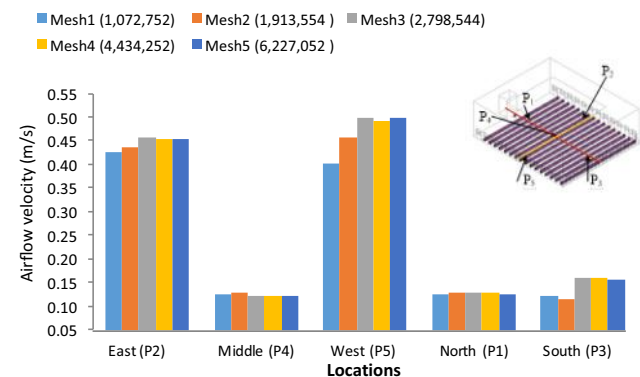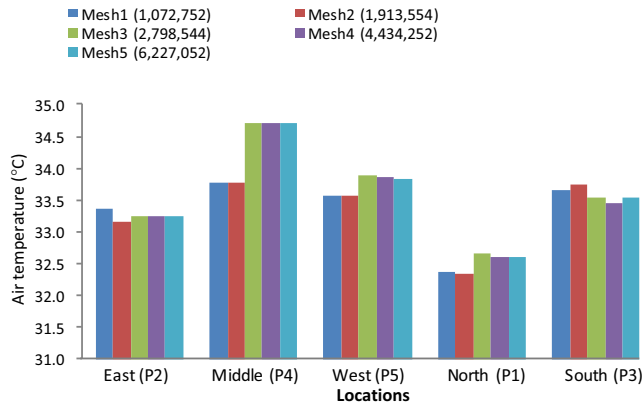

Fig. 9 Airflow velocity for different number of elements at the five data collection locations inside the mosque's hall.

Fig. 10 Air temperature for different number of elements at the five data collection locations inside the mosque's hall.

et al. [30]. Flow simulation was carried out on the baseline CFD model of the hall with boundary conditions and solution setup as described in Sections 2.3.3 and 2.3.4., respectively. Three meshing densities of the CFD model were considered, namely coarse meshing with 1,072,752 elements, medium meshing with 2,798,544 elements and fine meshing with 6,227,052 elements. For the fine meshing, the GCI was calculated using a formula

$$GCI_{fine} = \frac{F_s|\varepsilon|}{r^p - 1} \times 100 \quad (\%) \tag{5}$$

where F_s represents a safety factor, ε is a relative error, r is the grid refinement ratio, and p is an order of accuracy of the algorithm. The safety factor, F_s, was taken as 1.25 [30]. The value of relative error r was determined based on the ratio of number of elements, N for the fine and coarse meshing, as follows

$$r = \left(\frac{N_{fire}}{N_{coarse}}\right)^{\frac{1}{3}} \tag{6}$$

and the values of ε and p were determined using the following equations

$$\varepsilon = \frac{(f_2 - f_1)}{f_1} \tag{7}$$

$$p = \frac{\ln\left((f_3 - f_2)/(f_2 - f_1)\right)}{\ln(r)} \tag{8}$$

where f_1 denotes the solution for the fine grid, f_2 for the medium grid, and f_3 for the coarse grid. Two results of flow simulation were considered namely the airflow velocity and air temperature. The calculated GCI values for the airflow velocity and air temperature for the baseline CFD model of the mosque given in Table 5. The GCI of the airflow velocity

and air temperature are 0.0147% and 0.0228%, respectively. This finding shows that the flow simulation results for the baseline CFD model with the finest grid size are very close to their respective asymptotic values.

The quality of meshing for the baseline CFD model was evaluated based on values of mesh skewness, orthogonal quality and element quality. For good quality meshing, the element skewness should be close to zero while both the orthogonal quality and element quality should be close to unity. For the CFD model meshed with 2,798,544 elements, the skewness, orthogonal quality and element quality of was found to be 0.13, 0.97 and 0.98, respectively. A non-dimensional distance from the wall surface called the y^+ was in the range of $30 < y^+ < 300$, which are considered as excellent [37,38]. A summary of the mesh quality of the baseline CFD model of the hall is tabulated in Table 6.

2.3.8. Validation of the baseline CFD model
The baseline CFD model of the hall was validated by carrying out flow simulation with boundary conditions as described in Section 2.3.3 and solution setup described in Section 2.3.4. The *SST k-ω* turbulent flow model was employed to model the airflow while the species transport model was employed to model moisture transport in the air. The magnitudes of air temperature, airflow velocity and humidity at the five data collection locations inside the hall were observed at the end of the simulation. These data were compared to their respective values obtained from the field measurement, for April 2015. Fig. 11 shows plots of air temperature versus the measured values at all data collection locations. It can be observed that there is an excellent agreement between the simulated and measured air temperature, with percentage differences smaller than 2%. Fig. 12 shows a similar plot for the airflow velocities. There is also a satisfactory agreement between the predicted and measured airflow velocity, with percentage difference ranging from 7% to 18%. Fig. 13 illustrates the same plot for the air relative humidity. The percentage differences between the predicted and measured values are between 1% and 4.6%, which can also be considered as very good agreement.

2.4. Effects of exhaust fans on thermal comfort

The primary goal of this study is to improve the thermal comfort inside the mosque's hall by means of installing exhaust fans on the hall's envelope. This approach was chosen as it is economical, sustainable and more accessible to implement as compared to using other cooling methods. To find out the suitable number of fans to use and their location on the hall envelope, a parametric study was carried out. Four cases of fan number-location combination were considered, which are

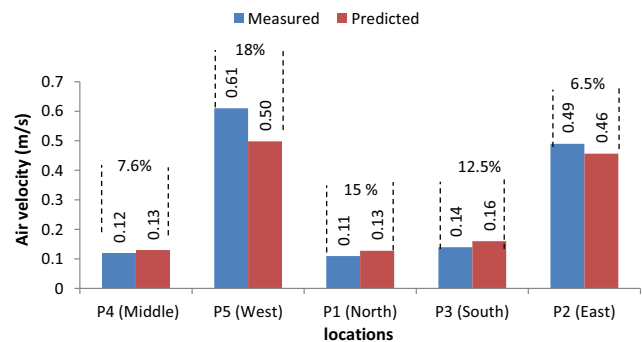**Table 5** The GCI values for baseline CFD model of the mosque.

	Refinement ratio (r)		Relative difference (ε)		Order of accuracy (p)		Grid Convergence Indexes (GCI)	
	r_{21}	r_{32}	ε_{21}	ε_{32}	p_{21}	p_{32}	GCI_{21}	GCI_{32}
Air velocity	1.376	1.305	−0.125	0.0037	11	13	0.47	0.0147
Air temperature	1.376	1.305	−0.0081	0.0007	6.7	8	0.168	0.0228

Table 6 Mesh quality of the baseline CFD model of the hall.

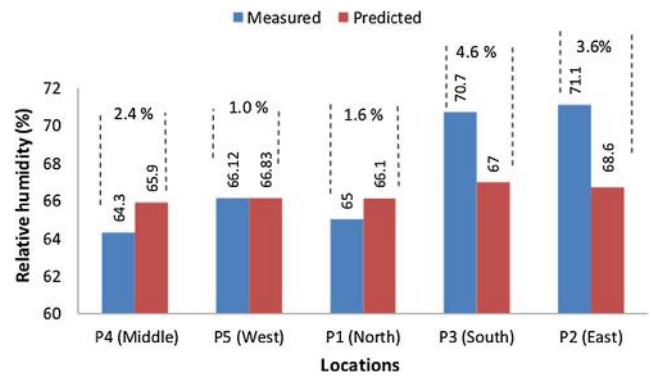| Size		Mesh metric	
Maximum	0.253 m	Skewness (close to 0.0)	0.13
Minimum	0.002 m	Orthogonal quality (close to 1.0)	0.97
Curvature normal angle	18°	Element quality (close to 1.0)	0.98
Growth rate	1:2	Non-dimensional number y+	30–77
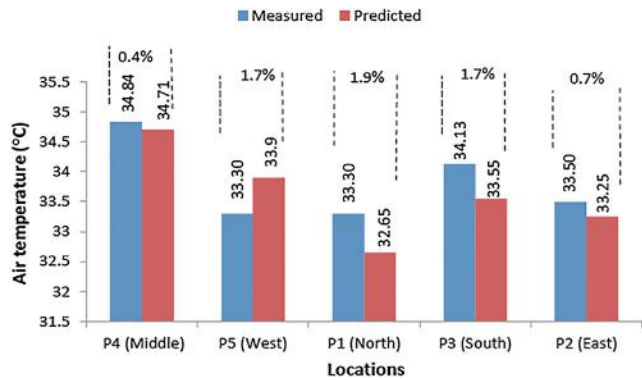
Fig. 11 Comparison of simulated and measured air temperatures at all data collection locations inside the mosque's hall.

Fig. 12 Comparison of simulated and measured airflow velocities at all data collection locations inside the mosque's hall.

Fig. 13 Comparison of simulated and measured relative humidity at all data collection locations inside the mosque's hall.

Table 7 Cases considered in the parametric study.

Cases	Locations	Number of fans	Airflow velocity
Case 1	Roof	12	$\bar{V} = 3.34$ m/s
Case 2	West-side wall	12	$\bar{V} = 3.34$ m/s
Case 3	East-side wall	12	$\bar{V} = 3.34$ m/s
Case 4	South-side wall	10	$\bar{V} = 4.0$ m/s

Table 8 Boundary conditions prescribed at the exhaust fans.

Section	Boundary conditions	Parameters
Exhaust fan	Mass flow rate	3.6 kg/s
	Air velocity	3–4 m/s
	Temperature	300 K
	Diameter	1 m
	Upper limit of absolute pressure	101.34 kPa
	Lower limit of absolute pressure	101.32 kPa
	Pressure jump coefficient	1

shown in Table 7. The airflow velocity at the exhaust fans is required as a boundary condition for the CFD flow simulation. Its magnitude was calculated based on the approximate volume of the hall and the air change rate (ACH) requirement for such space, as recommended in the ASHRAE Standard-55 [9]. The approximate volume of the mosque's main hall is 12,600 m³ while the air change rate per hour (ACH) was found to be between 8 and 12. The calculated airflow velocity of the exhaust fans is shown in Table 7, which were based on ACH value of 9. Based on the calculated airflow velocity, exhaust fans with a 1-m diameter were found to be suitable to be employed in this study. The complete boundary conditions specified at the exhaust fans are given in Table 8.

Fig. 14 shows the simplified geometries of the mosque's hall for the four cases shown in Table 7. The small hole features on the geometries represent the exhaust fans. CFD flow simulations were performed on each geometry with the boundary conditions and solution setup as described in Sections 2.3.3 and 2.3.4 above. The additional boundary condition for the inwards airflow velocity was prescribed at exhaust fan features.

The magnitudes of air temperature and airflow velocity at the five data collection locations were obtained from the results of the CFD flow analyses. They were then used to calculate the PMV and PPD thermal comfort indices at these locations. They were compared with the corresponding values calculated based on the air temperatures and airflow velocities obtained from the field measurement, for April 2015.

3. Results and discussion

3.1. Present thermal comfort condition

Fig. 15 shows plots of PMV values at all the data collection locations inside the mosque's hall for all the months, under the present ventilation condition. The PMV values were calculated based on the magnitudes of air temperature, airflow
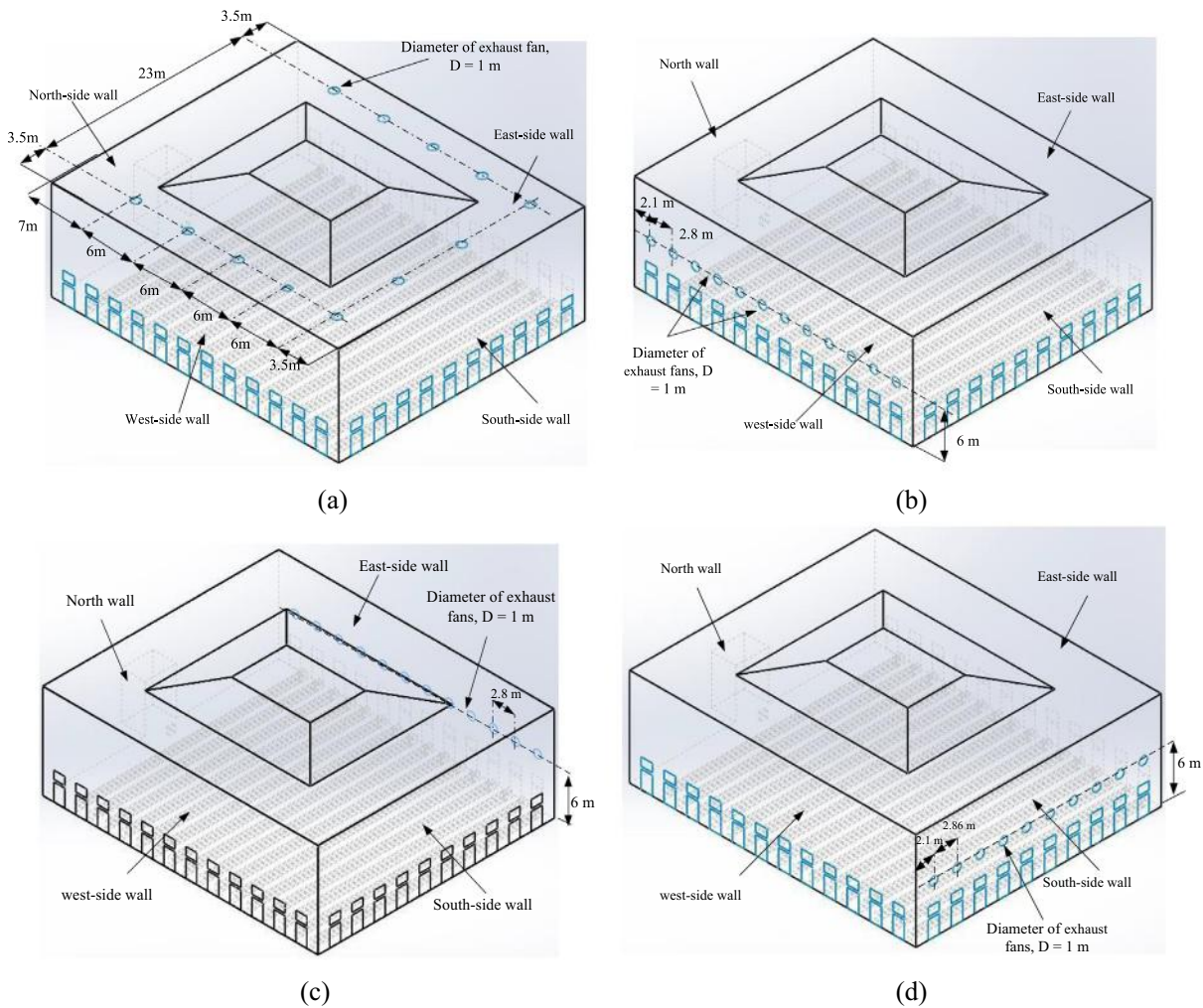
Fig. 14 Geometries of the mosque's hall for parametric study: (a) *Case 1*: 12 exhaust fans installed at the roof, (b) *Case 2*: 12 exhaust fans installed on west-side wall, (c) *Case 3*: 12 exhaust fans installed at the east-side wall, and (d) *Case 4*: 10 exhaust fans installed at the south-side wall.

velocity, and mean radiant temperature obtained from the field measurement, together with occupants' metabolic rate and clothing thermal resistance. The metabolic rate of the occupants was taken as 1.2 W/m^2, which corresponds to a sedentary activity. The clothing thermal resistance was assumed as 0.55 m^2 K/W [11]. It can be observed from the figure that for all the months, the PMV values at nearly all data collection locations inside the mosque's hall are higher than the upper limit of +0.5 as recommended by the ASHRAE Standard-55 [11]. This indicates that, under the present ventilation condition, the thermal comfort condition inside the mosque's hall is "warm." However, the PMV values for December 2014, January, February, and March 2015 at locations P1 (north), P2 (east) and P3 (south) are lower than +0.5. The PMV values are highest at the middle region of the hall, for all the months. This is expected because the middle region of the hall is far away from the doors and windows where there are flows of air. This causes very low airflow velocity and highest air temperature in this region. It is seen that the highest value of the PMV is +2.2, which occurs in April 2015.

Fig. 16 shows a similar plot for the PPD index under the present ventilation condition. The PPD values at nearly all data collection locations are higher than the upper limit of 10% as stipulated in the ASHRAE Standard-55 [11], especially for October, November 2014, April, May, July, August and September 2015. The highest PPD values occur in the middle region of the hall, for all the months. This is also expected for reasons similar to those stated earlier. The highest value of the PPD is 87%, which occur in April 2015.

Fig. 17 shows an hourly variation of the air temperature at all the data collection locations, for April 2015. It can be noticed that the lowest air temperature occurs in the region close to the north-side wall of the hall (location P1) while the highest temperature occurs in the region at the middle of the hall (location P4), which are far away from the doors and windows. The highest temperature occurs in between 1:30 PM and 1:50 PM, at all the data collection locations. Fig. 18 shows an hourly variation of the airflow velocity at all the data collection locations, for April 2015. It may be noticed that the airflow velocity is highly fluctuating in all
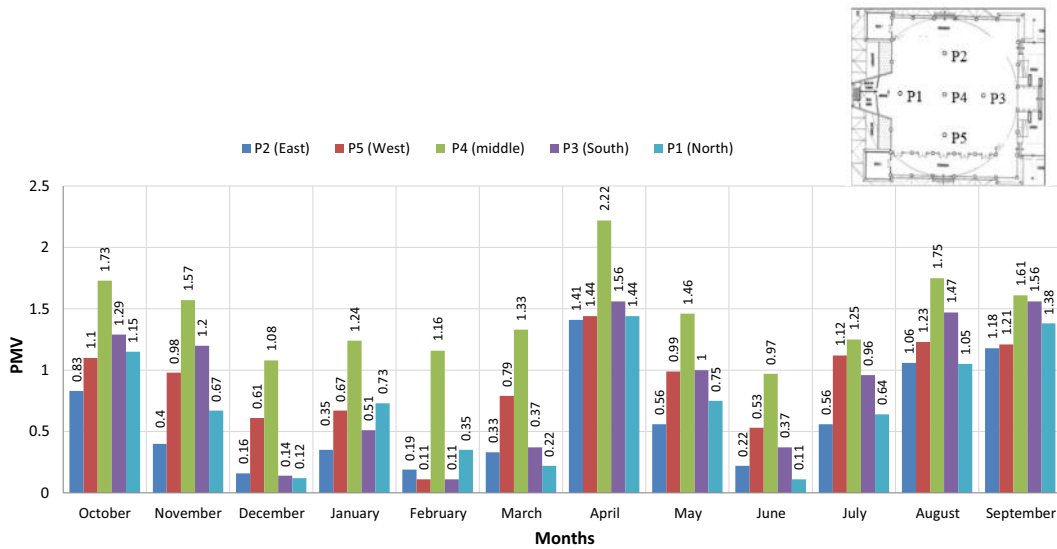
Fig. 15   PMV values at all data collection locations, for all the months, under the present ventilation.
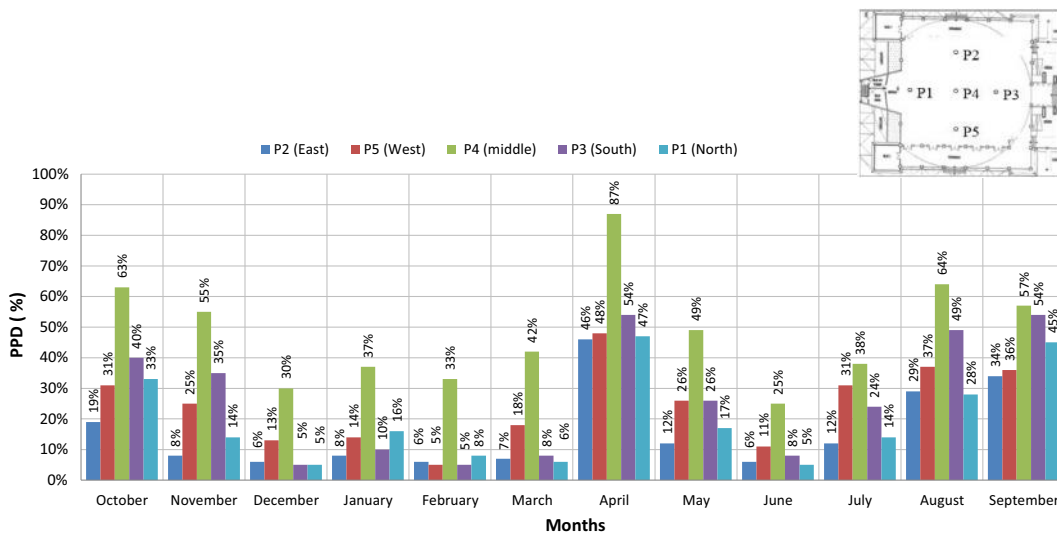

Fig. 16   PPD values at all data collection locations, for all the months, under the present ventilation.
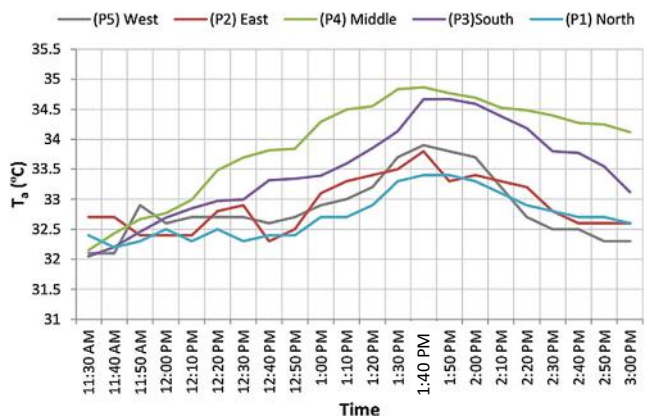

Fig. 17   Hourly variation of air temperature at all data collection locations for April 2015.

the locations. The highest reading of airflow velocity was in the region closed to the east-side wall (location P2) while the lowest reading was recorded in the middle region of the hall (location P4).

The values of PMV and PPD indices for April 2015, at all data collection locations under the present ventilation condition, are summarized in Table 9.

3.2. Effects of exhaust fans on airflow and temperature

Fig. 19 shows the spatial distribution of airflow velocity inside the mosque's hall, obtained from the CFD flow simulation, for the baseline CFD model, which is the one under the present ventilation condition. The plots shown are on two sectional planes, A-A and B-B, both of which pass through the middle region of the hall.
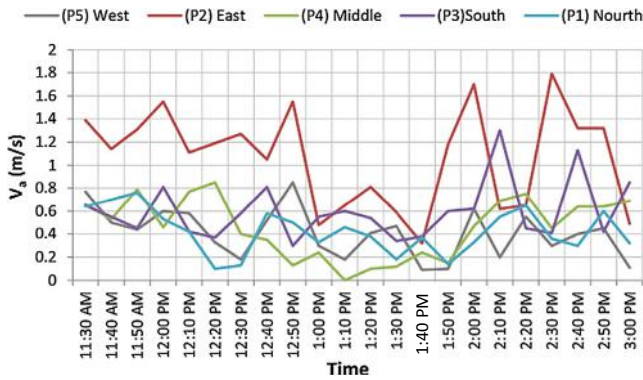
Fig. 18 Hourly variation of air velocity at all data collection locations for April 2015.

Table 9 PMV and PPD values in the month of April 2015.

Data collection locations	PMV	PPD
(ASHRAE)	(−0.5 to +0.5)	(10%)
P1 (north)	+1.44	47%
P2 (east)	+1.41	46%
P3 (south)	+1.56	54%
P4 (middle)	+2.22	87%
P5 (west)	+1.44	48%

PMV of -0.5 to +0.5 indicates good thermal comfort condition. PPD value of less than 10% shows the acceptable condition of thermal comfort.

It can be observed that the airflow velocity inside the hall, closed to the occupants who are in their sitting position, is generally lower than 0.3 m/s. As stated earlier, the effects of occupants breathing on the airflow velocity distribution were ignored in this study to simplify the CFD modeling and flow simulations. It is also seen that the airflow velocity becomes increasingly smaller in magnitudes at distances higher from the floor level. This is because, at these heights, there are no openings on the walls of the hall that could promote the flow of air. Fig. 20 shows the distribution of air temperature inside the mosque's hall from the CFD flow simulation, on the same sectional planes A-A and B-B. It is seen that, close to the sitting occupants, the air temperature is around 306 K (33 °C), which is considered high. Added with the fact that there is low airflow velocity in this region, the occupants would experience a very uncomfortable condition.

Fig. 21 shows the distribution of airflow velocity on the sectional planes A-A and B-B, for *Case 1*, in which twelve exhaust fans with a 1-m diameter are placed on the roof. Fig. 22 illustrates the corresponding air temperature distribution on the same sectional planes. One may notice that the added ventilation fans at the roof have a potential of increasing the airflow velocity and at the same time, reducing the air temperature in the region close to the occupants. These would help improve the thermal comfort condition inside the mosque's hall. It is seen that the airflow velocity in regions closed to the occupants' increases from about 0.13 m/s to 0.3 m/s, which is quite considerable. The air temperature in this region decreases from about 306 K (33 °C) to 302 K (29 °C).

The airflow velocity and air temperature at all five data collection locations were obtained from the results of the CFD
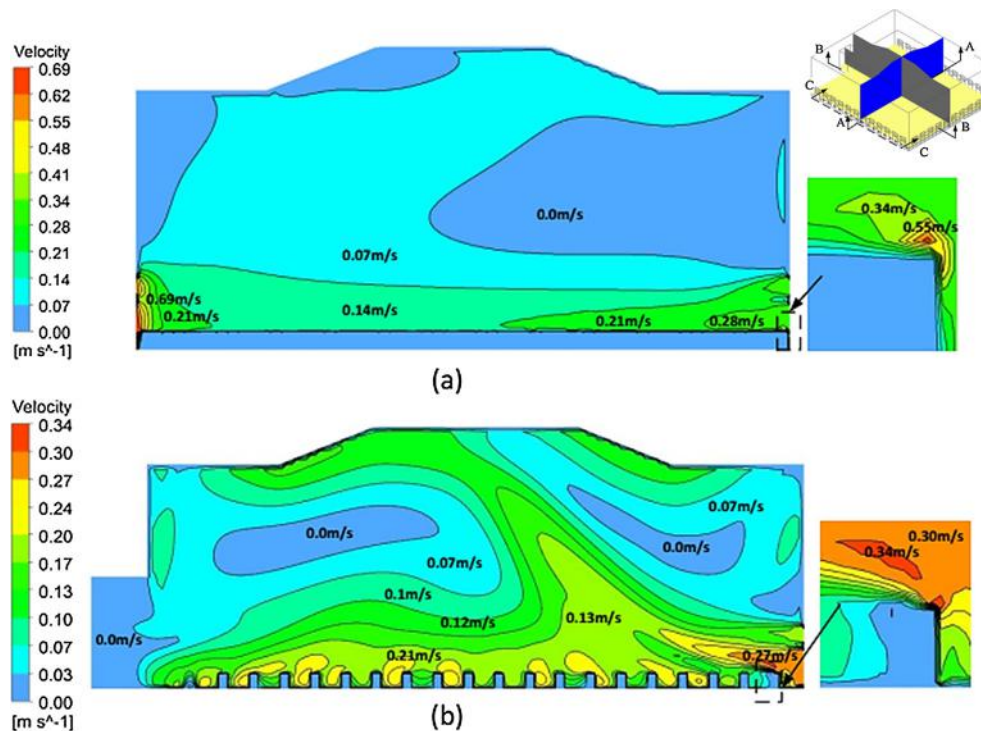
Fig. 19 Distribution of airflow velocity (in m/s) inside the mosque's hall for the baseline CFD model: (a) on a sectional plane A-A, and (b) on a sectional plane B-B.
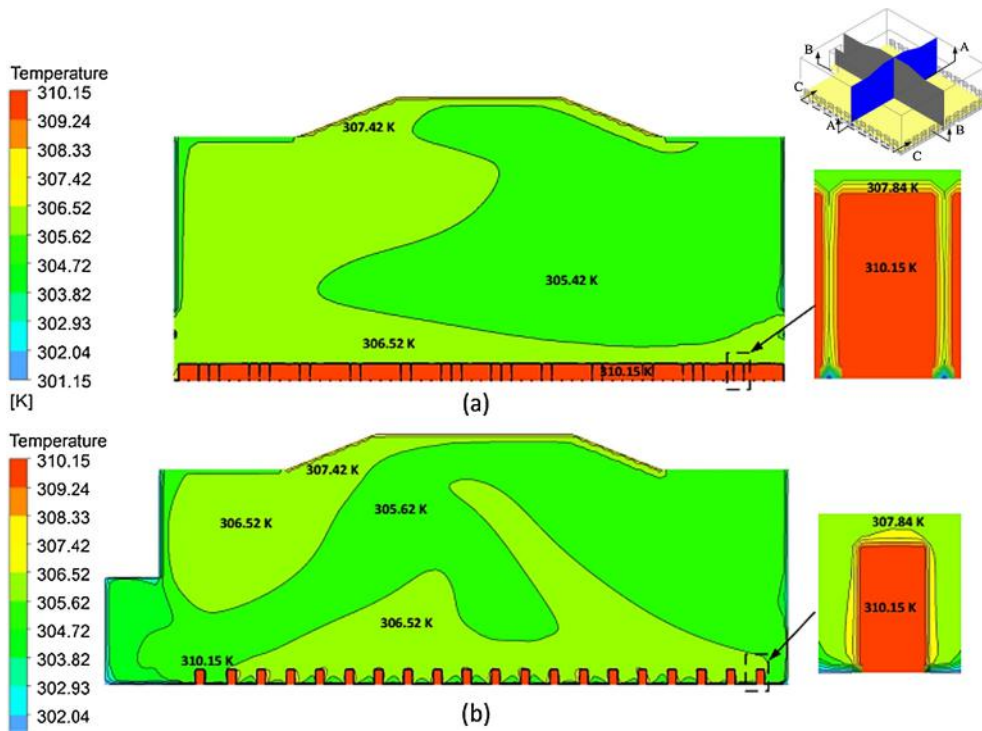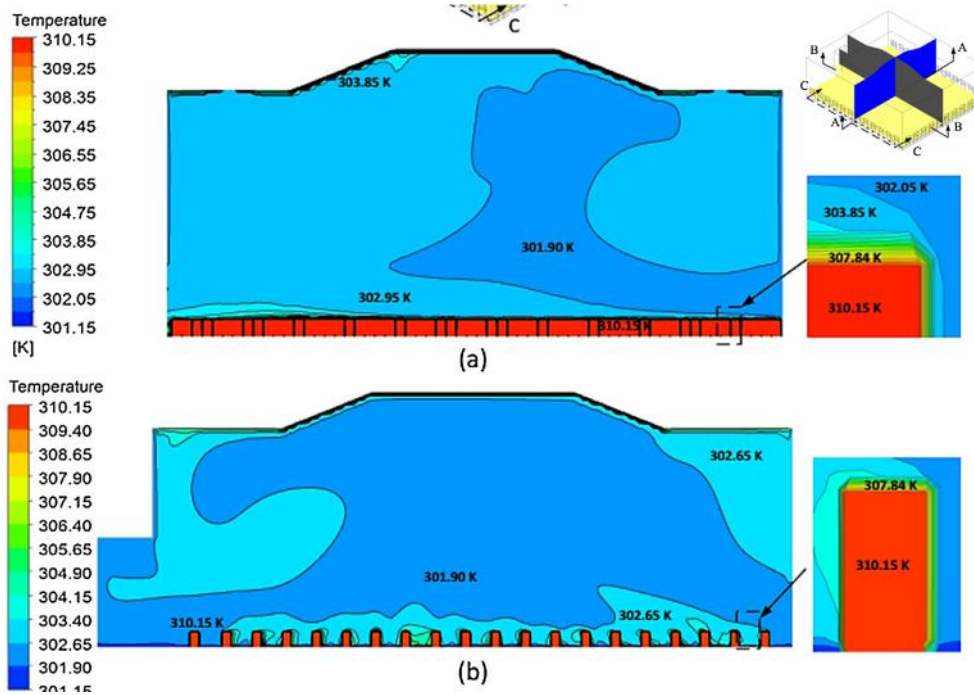
Fig. 20 Distribution of air temperature (in K) inside the baseline CFD model: (a) on a sectional plane A-A, and (b) on a sectional plane B-B.
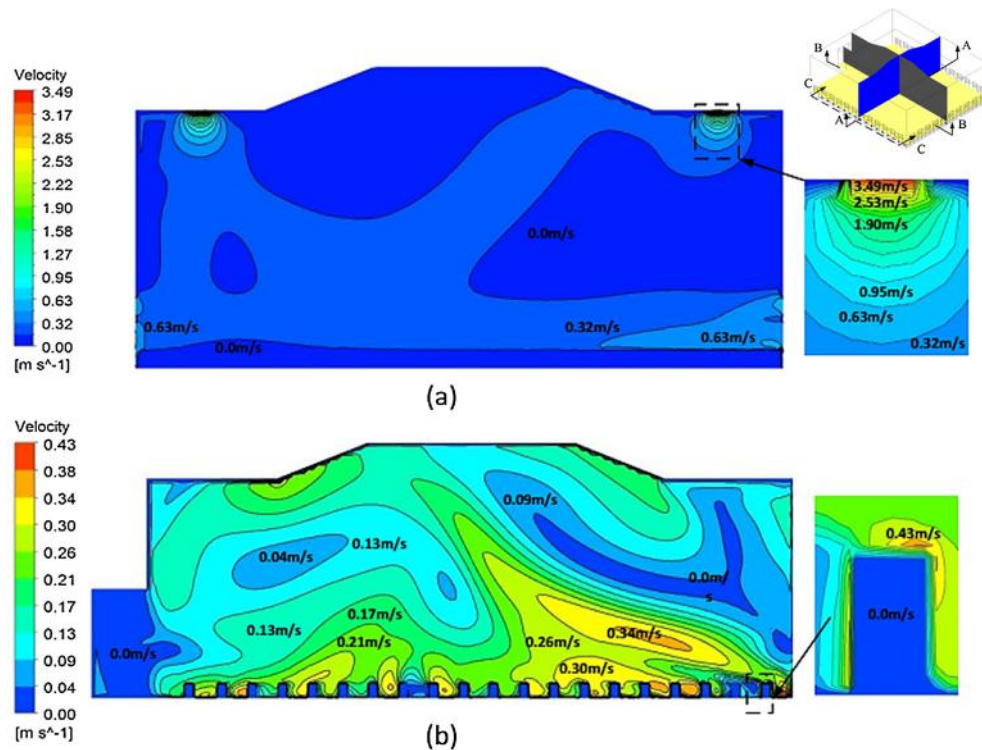
Fig. 21 Distribution of airflow velocity (in m/s) inside the hall for *Case 1* (12 exhaust fans placed at the roof): (a) on a plane A-A, and (b) on a plane B-B.

flow simulation. They were then used to compute the PMV and then PPD indices at these locations. Fig. 23 shows a plot

of PMV at all data collection locations for *Case 1* and their comparison with values calculated based on the field measure-

Fig. 22 Distribution of air temperature (in K) inside the hall for *Case 1* (12 exhaust fans placed at the roof): (a) on a plane A-A, and (b) on a plane B-B.
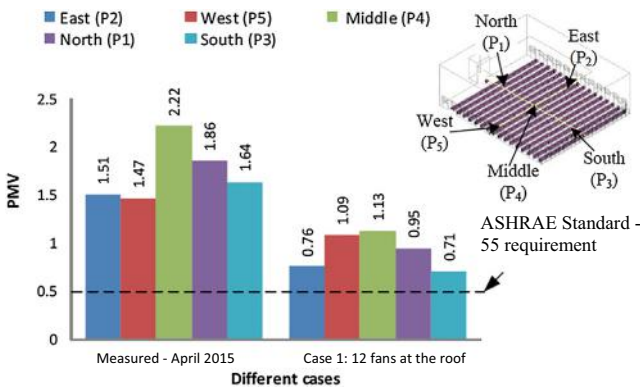
ment data for April 2015. This plot suggests that installing twelve 1-m diameter exhaust fans at the roof, with the arrangement shown in Fig. 14(a), would reduce the PMV index between 50% and 56%, relative to the present ventilation condition. This is a direct manifestation of the increase in airflow velocity and reduction in air temperature inside the hall, in the regions closed to the occupants.

The potential of reducing the PPD index in the same region of the hall is even more significant. This can be seen from the plot of the PPD index at all data collection locations as shown in Fig. 24. As seen from the figure, the PPD index in the region could potentially be reduced between 50% and 85% relative to the present ventilation condition.

Table 10 summarizes the percentage reduction in both the PMV and PPD indices at all the data collection locations, for *Case 1*. It can be seen that the highest reduction in both
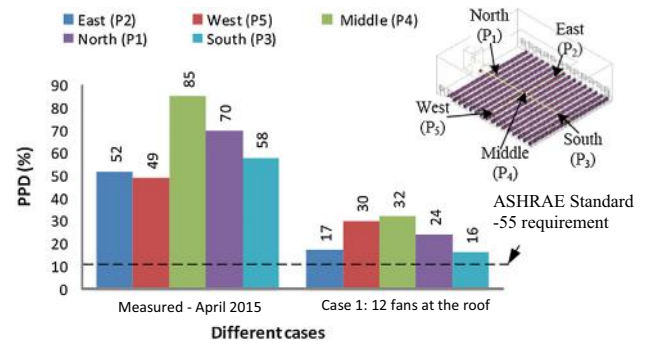
Fig. 24 Reduction in the PPD index at all data collection locations for *Case 1*.

the PMV and PPD indices occur at location P3, which is near to the south-side wall of the mosque's hall. On the other hand, the smallest reductions in both indices occur at location P5, which is near to the west-side wall of the hall. Although both the PMV and PPD indices were reduced quite significantly at all locations, their magnitudes are still higher than the respective upper limits specified in the ASHRAE Standard-55 [11].

The same CFD flow simulation was then repeated for the other case studies of exhaust fans installation. For each case, airflow velocities and air temperatures at the same locations were used to calculate the two thermal comfort indices. Fig. 25 shows the plots PMV index at all data collection locations for Case 2, Case 3, and Case 4. The PMV index at similar locations based on the field measurement data for April 2015 are also shown for comparison. It is seen that for all these cases the PMV index at all the data collection locations is reduced below the upper limit of +0.5 prescribed in the ASHRAE

Fig. 23 Reduction in the PMV index at all data collection locations for *Case 1*.

Table 10 Percentage reduction in the PMV and PPD indices for *Case 1*.

Data collection point	PMV (%)	PPD (%)
P1 (North)	48.9	65.7
P2 (East)	49.7	67.3
P3 (South)	56.7	72.4
P4 (Middle)	49.6	62.4
P5 (West)	25.9	38.8

Table 11 Percentage reductions in the PMV index for Case 2, Case 3 and Case 4.

Location	Case 2 (%)	Case 3 (%)	Case 4 (%)
P1 (North)	74.2	74.2	75.3
P2 (East)	84.8	67.5	95.4
P3 (South)	83.5	90.2	91.5
P4 (Middle)	77.9	78.4	78.4
P5 (West)	66.7	85.7	97.3
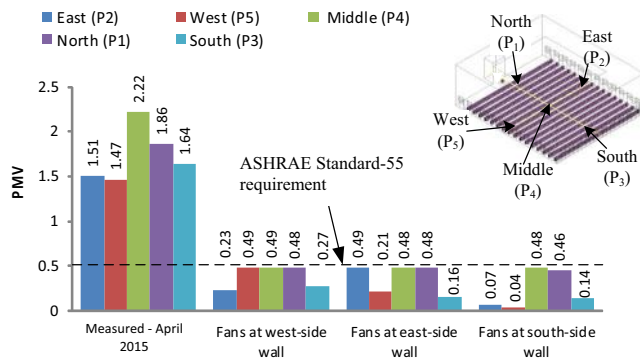
Fig. 25 PMV index at all data collection locations for Case 2, Case 3, and Case 4, and comparison with the corresponding values for the baseline case.

Table 12 Percentage reductions in the PPD index for Case 2, Case 3 and Case 4.

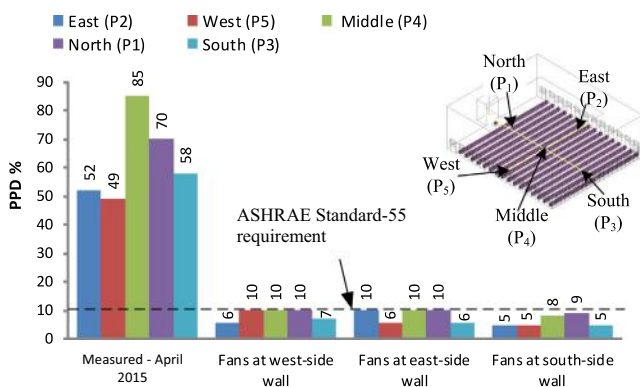| Location	Case 2 (%)	Case 3 (%)	Case 4 (%)
P1 (North)	85.7	85.7	87.1
P2 (East)	88.5	80.8	90.4
P3 (South)	87.9	89.7	91.4
P4 (Middle)	88.2	88.2	90.6
P5 (West)	79.6	87.8	89.8

Standard-55 [11]. This suggests that placing exhaust fans on the walls of the mosque's hall has a much more significant potential of improving the thermal comfort condition inside the mosque's hall as compared to installing the fans at the roof. It can also be noted that the most significant reduction in the PMV index can be attained in Case 4, when ten 1-m diameter exhaust fans are placed on the south-side wall of the hall, as shown in Fig. 14(d).

Fig. 26 shows plots of PPD index at all data collection locations inside the hall for Case 2, Case 3, and Case 4. The PPD index calculated based on the field measurement data for April 2015 at similar locations are also shown for comparison. As seen from this figure the PPD plots follow a similar trend to that of the PMV plots. The PPD index at all the locations

for all cases is reduced significantly to values below the upper limit of 10% as recommended in ASHRAE Standard-55 [11]. The most significant reduction of the PPD index occurs in Case 4 when ten 1-m diameter exhaust fans are placed at the south-side wall of the hall, as illustrated in Fig. 14(d).

Table 11 summarizes the percentage reductions in the PMV index at all data collection locations, for Case 2, Case 3 and Case 4. It can be observed that the most significant reduction in the PMV index is 97.3%, which occurs for Case 4, in the area near the west-side wall (location P5). The PMV index at this location is +0.04, which is close to an ideal thermal comfort condition based on the ASHRAE Standard-55 [11]. The percentage reductions in the PPD index at all data collection locations inside the mosque's hall, for Case 2, Case 3 and Case 4 are summarized in Table 12. It can be observed that, for Case 4, the most significant reduction in the PPD index is 91.4%, which occurs in the region close the south-side wall (location P3). The PPD index at this location is about 5%.

4. Conclusion

This study examines the state of thermal comfort inside the main hall of a mosque building under the present ventilation condition, as indicated by the PMV and PPD indices, calculated based on field data collected for a twelve-month duration. A computational fluid dynamic method was employed to examine the effects of installing exhaust fans on the thermal comfort condition inside the hall. Four cases of fan numbers-installation location combination were examined through a parametric study find out the one that would produce the most significant reductions in the PMV and PPD indices. It was found that, under the present ventilation condition, the PMV and PPD indices at five designated locations inside the hall exceed the respective upper limits as stated in the ASHRAE Standard-55. This indicates that the condition inside the hall is extremely uncomfortable for the occupants. It was also found that the use of exhaust fans having 1-m diameter has an excellent potential to increase airflow velocity and reduce

Fig. 26 PPD plots for Case 2, Case 3, and Case 4 and comparison with the corresponding values for the baseline case.

air temperature, thereby improving the thermal comfort in the regions closed to the sitting occupants. Finding from the parametric study suggests that installing ten exhaust fans on the south-side wall, at the height of 6 m from the floor, could reduce the PMV index between 75% and 95% and the PPD index between 87% and 91%. This translates into a very significant improvement in the thermal comfort condition inside the mosque's hall.

Acknowledgement

References

[1] P. Heiselberg, Ventilation of Large Spaces in Buildings, Aalborg Univ, Aalborg, Denmark, 1998.

[2] M.S. Al-Homoud, A.A. Abdou, I.M. Budaiwi, Assessment of monitored energy use and thermal comfort conditions in mosques in hot-humid climates, Energy Build. 41 (6) (2009) 607–614.

[3] P. Rajagopalan, M.B. Luther, Thermal and ventilation performance of a naturally ventilated sports hall within an aquatic centre, Energy Build. 58 (2013) 111–122.

[4] T.T. Xu, F.R. Carrié, D.J. Dickerhoff, W.J. Fisk, J. McWilliams, D. Wang, M.P. Modera, Performance of thermal distribution systems in large commercial buildings, Energy Build. 34 (3) (2002) 215–226.

[5] Q. Chen, Ventilation performance prediction for buildings: a method overview and recent applications, Build. Environ. 44 (4) (2009) 848–858.

[6] A. Merabtine, C. Maalouf, A.A.W. Hawila, N. Martaj, G. Polidori, Building energy audit, thermal comfort, and IAQ assessment of a school building: a case study, Build. Environ. 145 (2018) 62–76.

[7] K.M. Reena, A.T. Mathew, L. Jacob, A flexible control strategy for energy and comfort aware HVAC in large buildings, Build. Environ. (2018), 2018 Sept 13.

[8] I. El-Darwish, M. Gomaa, Retrofitting strategy for building envelopes to achieve energy efficiency, Alexandria Eng. J. 56 (4) (2017) 579–589.

[9] M.S. Bakhlah, A.S. Hassan, The study of air temperature when the sun path direction to Ka'abah: with a case study of Al-Malik Khalid Mosque, Malaysia, Int. Trans. J. Eng., Manage. Appl. Sci. Technol. 3 (2) (2012) 185–202.

[10] S.H. Ibrahim, A. Baharun, M.N.M. Nawi, E. Junaidi, Assessment of thermal comfort in the mosque in Sarawak, Malaysia, Int. J. Energy Environ. 5 (3) (2014) 327–334.

[11] American Society of Heating, Refrigerating, Air-Conditioning Engineers, & American National Standards Institute, Thermal Environmental Conditions for Human Occupancy, American Society of Heating, Refrigerating and Air-Conditioning Engineers, 2004.

[12] P.O. Fanger, Assessment of man's thermal comfort in practice, Occupat. Environ. Med. 30 (4) (1973) 313–324.

[13] G. Cao, H. Awbi, R. Yao, Y. Fan, K. Sirén, R. Kosonen, J.J. Zhang, A review of the performance of different ventilation and airflow distribution systems in buildings, Build. Environ. 73 (2014) 171–186.

[14] A.A.M. Elzaidabi, Low Energy, Wind Catcher Assisted Indirect-evaporative Cooling System for Building Applications (Doctoral dissertation), University of Nottingham, 2009.

[15] A.H. Abdullah, A Study on Thermal Environment Performance in Atria in the Tropics with Special Reference to Malaysia (Doctoral dissertation), Heriot-Watt University, 2007.

[16] P. Wouters, N. Heijmans, C. Delmotte, L. Vandaele, Classification of hybrid ventilation concepts, IEA Annex 35 (2) (1999).

[17] T. Kubota, D.T.H. Chyee, S. Ahmad, The effects of night ventilation technique on indoor thermal environment for residential buildings in hot-humid climate of Malaysia, Energy Build. 41 (8) (2009) 829–839.

[18] A.M.A. Rahman, H.L. Khalid, Y. Yusup, Optimizing wind power for energy efficient building design in tropical hot-humid climate of Malaysia, J. Sustain. Dev. 4 (2) (2011) 217.

[19] I. Hussein, M.H.A. Rahman, T. Maria, Field studies on thermal comfort of air-conditioned and non-air-conditioned buildings in Malaysia, in: Energy and Environment, 2009. ICEE 2009. 3rd International Conference on, IEEE, 2009, pp. 360–368.

[20] I.A. Raja, J.F. Nicol, K.J. McCartney, M.A. Humphreys, Thermal comfort: use of controls in naturally ventilated buildings, Energy Build. 33 (3) (2001) 235–244.

[21] Y. Zhai, H. Zhang, Y. Zhang, W. Pasut, E. Arens, Q. Meng, Comfort under personally controlled air movement in warm and humid environments, Build. Environ. 65 (2013) 109–117.

[22] N.H. Wong, J. Song, A.D. Istiadji, A study of the effectiveness of mechanical ventilation systems of a hawker center in Singapore using CFD simulations, Build. Environ. 41 (6) (2006) 726–733.

[23] S.C. Lee, M. Chang, Indoor and outdoor air quality investigation at schools in Hong Kong, Chemosphere 41 (1) (2000) 109–113.

[24] J. Khedari, N. Yamtraipat, N. Pratintong, J. Hirunlabh, Thailand ventilation comfort chart, Energy Build. 32 (3) (2000) 245–249.

[25] S. Atthajariyakul, C. Lertsatittanakorn, Small fan assisted air conditioner for thermal comfort and energy saving in Thailand, Energy Convers. Manage. 49 (10) (2008) 2499–2504.

[26] S.C. Sekhar, Space temperature difference, cooling coil and fan—energy and indoor air quality issues revisited, Energy Build. 37 (1) (2005) 49–54.

[27] W.K. Chow, W.Y. Fung, L.T. Wong, Preliminary studies on a new method for assessing ventilation in large spaces, Build. Environ. 37 (2) (2002) 145–152.

[28] S.H. Ibrahim, A. Baharun, M.M. Nawi, E. Junaidi, Analytical studies on levels of thermal comfort in typical low-income houses design, UNIMAS e-J. Civ. Eng. 5 (1) (2014) 28–33.

[29] A. Hussin, E. Salleh, H.Y. Chan, S. Mat, Thermal Comfort during daily prayer times in an Air-Conditioned Mosque in Malaysia, Proceedings of 8th Windsor Conference: Counting the Cost of Comfort in a Changing World, 2014.

[30] M. Hajdukiewicz, M. Geron, M.M. Keane, Calibrated CFD simulation to evaluate thermal comfort in a highly-glazed naturally ventilated room, Build. Environ. 70 (2013) 73–89.

[31] International Organization for Standardization, Ergonomics of the Thermal Environment: Analytical Determination and Interpretation of Thermal Comfort Using Calculation of the PMV and PPD Indices and Local Thermal Comfort Criteria, International Organization for Standardization, 2005.

[32] J.M. Villafruela, I. Olmedo, M.R. De Adana, C. Méndez, P.V. Nielsen, CFD analysis of the human exhalation flow using different boundary conditions and ventilation strategies, Build. Environ. 62 (2013) 191–200.

[33] C. Younes, C.A. Shdid, A methodology for 3-D multiphysics CFD simulation of air leakage in building envelopes, Energy Build. 65 (2013) 146–158.

[34] B. Sidawi, N. Hamza, K. Setaih, CFD modeling as a tool for assessing outdoor thermal comfort conditions in urban settings in hot arid climates, 2014.

[35] T. van Hooff, B. Blocken, L. Aanen, B. Bronsema, A venturi-shaped roof for wind-induced natural ventilation of buildings: wind tunnel and CFD evaluation of different design configurations, Build. Environ. 46 (9) (2011) 1797–1807.

[36] M.S.M. Ali, C.J. Doolan, V. Wheatley, Grid convergence study for a two-dimensional simulation of flow around a square cylinder at a low Reynolds number, in: P.J. Witt, M.P. Schwarz (Eds.), Seventh International Conference on CFD in The Minerals and Process Industries, 2009, pp. 1–6.

[37] P.J. Roache, Error bars for CFD, in: AIAA 41st Aerospace Sciences Meeting, 2003, p. 2003-0408.

[38] J.K. Calautit, D. O'Connor, P. Sofotasiou, B.R. Hughes, CFD simulation and optimisation of a low energy ventilation and cooling system, Computation 3 (2) (2015) 128–149;
A.N.S.Y.S. Fluent, ANSYS Fluent User's Guide, Release 14.0, ANSYS Fluent, PA, 2011.

[39] J.F. Nicol, I.A. Raja, A. Allaudin, G.N. Jamy, Climatic variations in comfortable temperatures: the Pakistan projects, Energy Build. 30 (3) (1999) 261–279.

[40] A.M. Abdul Rahman, Usaha-usaha Mencapai Keselesaan Terma Dalaman di Malaysia, 2000.

[41] Y.C. Tung, Y.C. Shih, S.C. Hu, Numerical study on the dispersion of airborne contaminants from an isolation room in the case of door opening, Appl. Therm. Eng. 29 (8) (2009) 1544–1551.

[42] K. Akbari, Impact of Radon Ventilation on Indoor Air Quality and Building Energy Saving (Doctoral dissertation), Mälardalen University, 2009.

[43] A.N.Z. Sanusi, Low energy ground cooling system for buildings in hot and humid Malaysia, 2012.

[44] S. Hussain, Numerical investigations of the indoor thermal environment in atria and of the buoyancy-driven ventilation in a simple atrium building (Doctoral dissertation), Queen's University (Canada), 2012.

[45] H.G. Tao, H.X. Chen, J.L. Xie, J.Z. Jiang, Comparison on simulation and experiment of supply air through metro vehicle air conditioning duct, in: Applied Mechanics and Materials, Trans Tech Publications, 2011, pp. 1724–1728.

[46] M. Woloszyn, T. Kalamees, M.O. Abadie, M. Steeman, A.S. Kalagasidis, The effect of combining a relative-humidity-sensitive ventilation system with the moisture-buffering capacity of materials on indoor climate and energy efficiency of buildings, Build. Environ. 44 (3) (2009) 515–524.

[47] J.W. Axley, Application of Natural Ventilation for US Commercial Buildings–Climate Suitability, Design Strategies & Methods, Modelling Studies, Gaithersburg, MD, NIST, 2001.

[48] G. Ye et al, A new approach for measuring predicted mean vote (PMV) and standard effective temperature (SET*), Build. Environ. 38 (2003) 33–44.